

# Quantum treatment of cavity-assisted entanglement of three-level atoms and two fields in an electromagnetically-induced-transparency configuration

Xihua Yang <sup>1,2,\*</sup>, Nicholas Brewer,<sup>1</sup> and Paul D. Lett <sup>1,3,†</sup>

<sup>1</sup>Joint Quantum Institute, National Institute of Standards and Technology and University of Maryland, College Park, Maryland 20742, USA

<sup>2</sup>Department of Physics, Shanghai University, Shanghai 200444, China

<sup>3</sup>Quantum Measurement Division, National Institute of Standards and Technology, Gaithersburg, Maryland 20899, USA



(Received 22 April 2021; revised 14 January 2022; accepted 24 January 2022; published 15 February 2022)

We examine the field-field and field-atom entanglements generated by  $\Lambda$ -type three-level atoms placed in an optical cavity driven above threshold by two coherent input optical fields. It is shown that under realistic experimental conditions entanglement between the two output cavity fields as well as between the fields and the atoms can be achieved when the two cavity fields are both one- and two-photon (Raman) resonant with the atomic transitions, as in the configuration for electromagnetically induced transparency (EIT). The entanglement has similar features to pump-signal-idler three-color entanglement in an above-threshold optical parametric oscillator [Villar *et al.*, *Phys. Rev. Lett.* **97**, 140504 (2006)]. This cavity-enhanced atom-field cooperative coupling could enable convenient and efficient generation of bright, nondegenerate, narrow-band entangled fields, which may find potential applications in realistic quantum communications and networking protocols.

DOI: [10.1103/PhysRevA.105.023711](https://doi.org/10.1103/PhysRevA.105.023711)

## I. INTRODUCTION

Entanglement, as one of the most intriguing features of quantum mechanics, is at the heart of quantum networks and quantum information processing. A common way to generate entanglement is to use parametric down-conversion processes in nonlinear optical crystals [1–4]; however, the entangled fields that are produced normally have large bandwidths and short correlation times. In order to reduce the bandwidth, an optical parametric oscillator (OPO) containing the optical crystal can be used and driven either below or above threshold [5–8]. Atomic systems in free space [9–15], cavity optomechanical systems [16–18], and atom-cavity hybrid systems [19–21], all interacting with light fields, can also be used to generate nondegenerate and narrow-bandwidth entangled fields. In comparison with a single-pass interaction scheme in free space, an optical cavity can dramatically enhance the light-matter interaction, and subsequently enhance the generated squeezing or entanglement [15–23].

Practical quantum communication networks would be composed of many quantum nodes and channels, where nondegenerate bright entangled fields with narrow bandwidth will be required to connect with many of the variety of physical systems, atoms, or ions, that could be present at the quantum nodes [12]. The atomic system interacting with light fields provides a promising interface for realizing various quantum information protocols, where light fields act as the long-distance quantum information carriers and the atomic ensemble acts as a quantum processor for storage and manipulation of quantum information [24,25]. The atomic coherence

decay time between the lower doublet of a  $\Lambda$ -type atomic level system is relatively long (on the order of tens of ms or more [26,27]), and makes it attractive for quantum memory applications [28].

In most of the previous studies on light-matter interactions, the relatively strong pump field is considered as a classical field and its quantum properties are ignored. In order to fully describe the quantum features of the light-matter interaction, however, all of the light fields should be treated quantum mechanically. Including the quantum nature of the strong pump field, Villar *et al.* demonstrated the production of pump-signal-idler three-color entanglement in an above-threshold optical parametric oscillator (OPO) [7,8]. Recently, the same group experimentally observed quantum correlations between twin beams that are produced by nondegenerate four-wave mixing with <sup>85</sup>Rb atoms when operating in an OPO above threshold [20]. This group has also presented a versatile model for exploring the multipartite entanglement among the strong pump field and the converted fields in open cavity (high transmission) OPOs for the doubly and triply resonant cavity configurations [21]. Moreover, they reported the experimental observation of intensity correlations and anticorrelations between the pump and probe fields in the simplest  $\Lambda$ -type three-level atomic system [29,30] and pointed out that quantum correlated intensities and anticorrelated phases of the pump and probe fields would exist at an analysis frequency inside the electromagnetically-induced-transparency (EIT) window in their system [31]. However, as demonstrated in Refs. [32,33], no quantum correlation or entanglement can exist in the traditional EIT configuration when the two fields interacting with the  $\Lambda$ -type three-level atom are treated classically.

By combining the virtues of the cavity-enhanced atom-field cooperative coupling with the full quantum mechanical

\*yangxh@shu.edu.cn

†lett@umd.edu

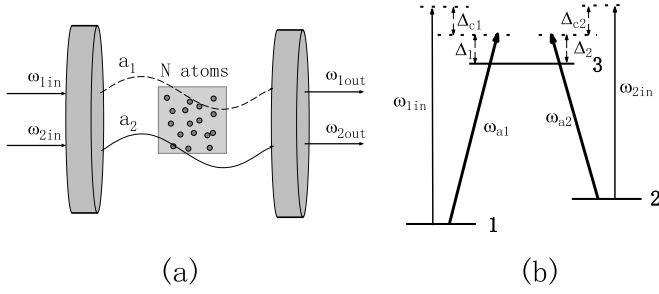


FIG. 1. (a) The optical cavity containing  $N$   $^{85}\text{Rb}$  atoms driven by two input laser fields with frequencies  $\omega_{1\text{in}}$  and  $\omega_{2\text{in}}$ , where  $a_1$  and  $a_2$  represent the two longitudinal cavity field modes with frequencies  $\omega_{a1}$  and  $\omega_{a2}$ , respectively. (b) The relevant energy level scheme of the  $\Lambda$ -type three-level  $^{85}\text{Rb}$  atoms and corresponding frequency detunings of the two cavity fields with respect to the input laser fields as well as the atomic resonant transitions.

treatment for both the atomic and field fluctuations, we show in the present work that entanglement between two bright output cavity fields, as well as between the output cavity fields and the atoms in the cavity, can be realized. We consider an optical cavity containing  $\Lambda$ -type three-level atoms when the two cavity fields are both one- and two-photon (Raman) resonant to the atomic transitions under realistic experimental conditions. This method could simplify the generation of bright, nondegenerate, narrowband entangled fields, which is vital to a number of practical quantum communications and networking tasks requiring coupling to atoms.

## II. THEORETICAL MODEL AND HEISENBERG-LANGEVIN EQUATIONS

We consider an ensemble of  $N$  cold atoms with a  $\Lambda$ -type energy level configuration (e.g.,  $^{85}\text{Rb}$ ) placed inside an optical cavity with the cavity length  $L$ , decay rate  $\kappa$ , and finesse  $F = \frac{\pi c}{L\kappa}$ , as shown in Fig. 1(a). The atom-cavity hybrid system is driven by two input laser fields with frequencies  $\omega_{1\text{in}}$  and  $\omega_{2\text{in}}$  coupling two neighboring longitudinal cavity modes with frequencies  $\omega_{a1}$  and  $\omega_{a2}$ , and the two cavity fields couple the atomic resonant transitions 1–3 and 2–3. The levels 1, 2, and 3 correspond here to the ground-state hyperfine levels  $5S_{1/2}(F=2)$ ,  $5S_{1/2}(F=3)$  and the excited state  $5P_{1/2}$  of the  $D_1$  line of the  $^{85}\text{Rb}$  atom, respectively, as displayed in Fig. 1(b). In this case, the total Hamiltonian of the hybrid system can be written as [19,22,23]

$$\begin{aligned}
 H = & \hbar\omega_{a1}a_1^\dagger a_1 + \hbar\omega_{a2}a_2^\dagger a_2 + i\hbar E_1(a_1^\dagger e^{-i\omega_1 \text{in}t} - a_1 e^{i\omega_1 \text{in}t}) \\
 & + i\hbar E_2(a_2^\dagger e^{-i\omega_2 \text{in}t} - a_2 e^{i\omega_2 \text{in}t}) + \hbar\omega_1\sigma_{11} + \hbar\omega_2\sigma_{22} \\
 & + \hbar\omega_3\sigma_{33} + (\hbar g_{13}\sqrt{N}a_1^\dagger\sigma_{13} + \hbar g_{23}\sqrt{N}a_2^\dagger\sigma_{23} + \text{H.c.}), \quad (1)
 \end{aligned}$$

where  $a_i$  ( $a_i^\dagger$ ) ( $i = 1, 2$ ) are the annihilation (creation) operators of the two cavity fields with decay rates  $\kappa_i$ . The two terms involving  $E_i = \sqrt{2P_i\kappa/\hbar\omega_{i\text{in}}}$  describe the interactions of the two input laser fields of power  $P_i$  with the two cavity modes (here we assume  $\kappa_1 = \kappa_2 = \kappa$ ).  $\sigma_{ab} = \frac{1}{\sqrt{N}} \sum_{i=1}^N \sigma_{ab}^{(i)}$  ( $a \neq b$ ,  $a, b = 1, 2, 3$ ) and  $\sigma_{aa} = \sum_{i=1}^N \sigma_{aa}^{(i)}$  are the collective operators of the atomic ensemble.  $g_{i3} =$

$\mu_{i3} \varepsilon_i/\hbar$  is the atom-field coupling constant with  $\mu_{i3}$  being the dipole moment for the  $i = 1, 2$  to 3 transitions.  $\varepsilon_i = \sqrt{\hbar\omega_{ai}/2\epsilon_0 V}$  is the electric field of a single cavity field photon with the free space permittivity  $\epsilon_0$  and cavity mode volume  $V = r^2 L$  (with beam radius  $r$ ). In our configuration, with suitably chosen experimentally available parameters, we consider cold atoms in a Fabry-Perot cavity and the condition where the interatomic separation is far larger than the resonant optical wavelength, so that the direct (or dipole-dipole) interaction between the atoms can be safely ignored in the above Hamiltonian in Eq. (1). By transforming the total cavity field  $E_i$  and the atomic operators  $\sigma_{ij}$  using a rotating wave approximation at the input field frequency  $\omega_{i\text{in}}$ , the Heisenberg-Langevin evolution equations for the collective atomic operators and cavity field operators for the Hamiltonian in Eq. (1), adding damping and dephasing terms, are given by

$$\dot{a}_1 = -(\kappa_1 + i\Delta_{c1})a_1 + E_1 - ig_{13}\sqrt{N}\sigma_{13} + \sqrt{2\kappa_1}a_1^{\text{in}}, \quad (2a)$$

$$\dot{a}_2 = -(\kappa_2 + i\Delta_{c2})a_2 + E_2 - ig_{23}\sqrt{N}\sigma_{23} + \sqrt{2\kappa_2}a_2^{\text{in}}, \quad (2b)$$

$$\begin{aligned} \dot{\sigma}_{12}(t) = & -[\gamma_{12} + i(\Delta_{c1} - \Delta_1 + \Delta_2 - \Delta_{c2})]\sigma_{12} + ig_{13}a_1\sigma_{32} \\ & - ig_{23}a_2^\dagger\sigma_{13} + F_{12}, \end{aligned} \quad (2c)$$

$$\begin{aligned} \dot{\sigma}_{13}(t) = & -[\gamma_{13} + i(\Delta_{c1} - \Delta_1)]\sigma_{13} - ig_{13}a_1(\sigma_{11} - \sigma_{33})/\sqrt{N} \\ & - ig_{23}a_2\sigma_{12} + F_{13}, \end{aligned} \quad (2d)$$

$$\begin{aligned} \dot{\sigma}_{23}(t) = & -[\gamma_{23} + i(\Delta_{c2} - \Delta_2)]\sigma_{23} - ig_{23}a_2(\sigma_{22} - \sigma_{33})/\sqrt{N} \\ & - ig_{13}a_1\sigma_{21} + F_{23}, \end{aligned} \quad (2e)$$

where  $\Delta_{ci} = \omega_{ai} - \omega_{i\text{in}}$  ( $\Delta_1 = \omega_{a1} - \omega_{31}$  and  $\Delta_2 = \omega_{a2} - \omega_{32}$ ) are the frequency detunings of the two cavity fields  $E_i$  with respect to the corresponding input laser fields (and the atomic 1–3 and 2–3 resonant transitions), respectively.  $a_i^{\text{in}}(t)$  are the optical noise operators with the relevant nonzero correlation functions  $\langle a_i^{\text{in}}(t)a_i^{\text{in}\dagger}(t') \rangle = \delta(t-t')$ .  $\gamma_{13} = \gamma_{23} = \frac{\gamma_1 + \gamma_2}{2}$  with the  $\gamma_i$  being the population decay rates (multiplied by branching fractions) from level 3 to levels 1 and 2 (normally of the order  $10^6 \text{ s}^{-1}$ ), respectively.  $\gamma_{12}$  is the coherence decay rate between levels 1 and 2 due to the finite interaction time between atoms and light beams (normally of the order of  $10^3 \text{ s}^{-1}$ ), and the  $F_{ij}(t)$  are the  $\delta$ -correlated collective atomic Langevin noise operators.

In order to study the quantum effects involving the two cavity fields as well as the atoms, one can write each atomic and cavity field operator as the sum of its mean value and a quantum fluctuation term (i.e.,  $\sigma_{ij} = \langle \sigma_{ij} \rangle + \delta\sigma_{ij}$  and  $a_i = \langle a_i \rangle + \delta a_i$ ). As discussed in Ref. [21], it is expected that this linearization may fail close to or below the oscillation threshold [34], and if that is the case, one can go beyond the linear treatment and investigate the entanglement properties by solving the Fokker-Planck equation for the nonlinear systems, as done in Refs. [34,35]. Here, we focus on the entanglement generation in an above-threshold optical parametric oscillator. We assume that the two cavity fields have equal power, the atomic lower doublet states have a long lifetime as compared to the excited state ( $\gamma_1, \gamma_2 \gg \gamma_{12}$ ), and the pumping rate  $\Gamma_i = g_{i3}^2 | \langle a_i \rangle |^2 / \gamma_i$  is much larger than  $\gamma_{12}$

(i.e., in the EIT regime) and smaller than  $\gamma_1, \gamma_2, \kappa$ . In this case, the atoms are pumped into the dark state formed by the lower doublet states 1 and 2 (i.e., the population in the excited state 3 can be neglected), and the optical coherences  $\sigma_{13}$  and  $\sigma_{23}$  adiabatically follow the ground-state observables. The two cavity fields are both one- and two-photon resonant with the  $\Lambda$ -type three-level atoms and we can analytically derive the steady-state mean values of the two cavity fields and the atomic operators by setting the time derivatives equal to zero and neglecting the noise operators. The phase references of the two driving fields are chosen to let  $\langle a_1 \rangle$  and  $\langle a_2 \rangle$  be real and positive. Under the situations that  $P_{1\text{in}} = P_{2\text{in}}$ , and  $\frac{2\kappa\langle a_i \rangle^2}{N\gamma_{12}} \gg \frac{1}{C_i}$ , where the cooperativity parameter  $C_i = g_{i3}^2 N / \kappa \gamma_i$  quantifies the strength of the atom-field cavity coupling, we find  $\langle a_i \rangle = (E_i \pm \sqrt{E_i - \kappa N \gamma_{12}}) / 2\kappa$  (see the Appendix for more details). It can be seen from the steady-state values that the intracavity fields exhibit bistable behavior when the input field power is larger than the threshold power  $P_{i\text{in}}^{\text{th}} = \hbar \omega_i \text{in} \gamma_{12} N$ . Under realistic experimental conditions,  $E_i \gg \kappa \gamma_{12} N$ , and we can safely take only the positive sign in the relation above and let  $\langle a_i \rangle = (E_i + \sqrt{E_i - \kappa N \gamma_{12}}) / 2\kappa$ . Using the input-output relation [12],

$$\langle a_i^{\text{out}} \rangle = \sqrt{2\kappa} \langle a_i \rangle - \langle a_i^{\text{in}} \rangle, \quad (3)$$

the output field power  $P_{i\text{out}}$  with respect to the input laser power  $P_{i\text{in}}$  can be obtained,

$$P_{i\text{out}} = P_{i\text{in}} - P_{i\text{in}}^{\text{th}}, \quad (4)$$

where the “th” superscript indicates the threshold value. The output power exhibits a linear response in the above-threshold regime. Similar linear response has been observed in an open cavity OPO for a doubly resonant cavity configuration [21].

By defining the cavity field fluctuation quadratures  $\delta X_i = (\delta a_i + \delta a_i^\dagger) / \sqrt{2}$  and  $\delta Y_i = (\delta a_i - \delta a_i^\dagger) / \sqrt{2}i$  with the corresponding Hermitian input noise operators  $\delta X_i^{\text{in}} = (\delta a_i^{\text{in}} + \delta a_i^{\text{in}\dagger}) / \sqrt{2}$  and  $\delta Y_i^{\text{in}} = (\delta a_i^{\text{in}} - \delta a_i^{\text{in}\dagger}) / \sqrt{2}i$ , the atomic quadratures  $\delta X_a = (\delta \sigma_{12} + \delta \sigma_{21}) / \sqrt{2}$  and  $\delta Y_a = (\delta \sigma_{12} - \delta \sigma_{21}) / \sqrt{2}i$  with the corresponding Hermitian noise operators  $X_s^{\text{in}} = (F_{21} + F_{12}) / \sqrt{2}$  and  $Y_s^{\text{in}} = (F_{12} - F_{21}) / \sqrt{2}i$ . By eliminating the excited-state population as well as replacing the optical coherences  $\sigma_{13}$  and  $\sigma_{23}$  with their steady-state values, one can obtain the quantum Langevin equations for the fluctuation operators. (In linearizing, we have ignored terms of the form  $\delta a \delta \sigma$ .) Taking the Fourier transform of these equations, the quantum fluctuations of the operators with respect to the Fourier frequency  $\omega$  can be obtained. The fluctuations of the output fields can be obtained by using the input-output relation [12]:

$$\delta A_i^{\text{out}}(\omega) = \sqrt{2\kappa} \delta A_i(\omega) - A_i^{\text{in}}(\omega) \quad (A = X, Y). \quad (5)$$

We employ the Duan-Giedke-Cirac-Zoller (DGCZ) criterion of Ref. [36] to test for entanglement between the two output cavity fields, as well as between the fields and the atomic spin coherence. The DGCZ criterion can be expressed as  $V = (\Delta U)^2 + (\Delta V)^2 > 2$ , where  $U = X_1 \pm X_2$  and  $V = P_1 \mp P_2$  with the quadratures  $X_i = (a_i + a_i^\dagger) / \sqrt{2}$  and  $Y_i = (a_i - a_i^\dagger) / \sqrt{2}i$  being Einstein-Podolsky-Rosen (EPR) type operators. In the frequency domain, the criterion can be written as [37]

$$V = \langle \delta U(\omega) [\delta U(\omega)]^\dagger + \delta V(\omega) [\delta V(\omega)]^\dagger \rangle > 2, \quad (6)$$

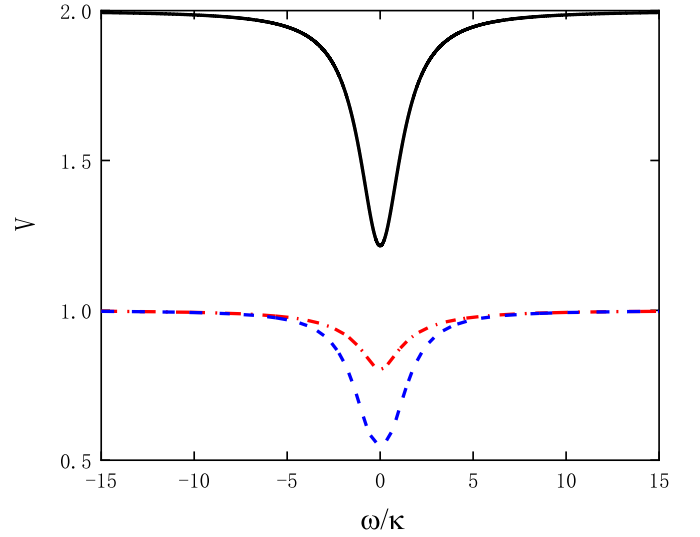


FIG. 2. The correlations  $V_{12}$  (solid black line),  $V_{1a}$  (dot-dashed red line), and  $V_{2a}$  (dashed blue line) as a function of the Fourier frequency  $\omega$  (normalized to the cavity decay rate  $\kappa$ ).  $V_{12}$  represents the correlation between the two output cavity fields, and  $V_{1a,2a}$  represents the correlation between the output cavity field 1 (2) and the atoms. The relevant parameters are given in the text.

where  $\delta U = \delta X_i \pm \delta X_j$  and  $\delta V = \delta Y_i \mp \delta Y_j$  ( $i, j = 1, 2, a$ ; taking the upper sign for  $V_{12}$  and  $V_{1a}$ , and the lower sign for  $V_{2a}$ ). If the above inequality is violated, then the bipartition is necessarily entangled, and in this case the smaller the correlation  $V$ , the stronger the degree of the entanglement. Note that similar entanglement properties can also be deduced using the criterion of the inferred variances described in Ref. [38]. In the following the parameters of the cavity-atom hybrid system are similar to those in the experiments of Ref. [39], and are set to  $L = 0.05$  m,  $r = 200$   $\mu\text{m}$ ,  $N = 10^4$ ,  $F = \frac{\pi c}{L\kappa} = 100$ ,  $\lambda = 795$  nm,  $\gamma_1 = \gamma_2 = 2\pi \times 3 \times 10^6$  s $^{-1}$ ,  $\gamma_{12} = 2\pi \times 10^3$  s $^{-1}$ ,  $\omega_{12} = 2\pi \times 3$  GHz,  $P_1 = P_2 = 1$   $\mu\text{W}$  and  $\Delta_1 = \Delta_2 = \Delta_{c1} = \Delta_{c2} = 0$ . The cavity length of 0.05 m implies a free spectral range (FSR) of about 3 GHz, approximately corresponding to the hyperfine splitting of the ground state of the  $^{85}\text{Rb}$  atoms, which enables the simultaneous satisfaction of the one- and two-photon resonance conditions for the two cavity fields with respect to the atomic transitions. We consider cold atoms in the Fabry-Perot cavity and the atom number given here would fit in a laser dipole trap. We did not consider hot atoms, as in this case the Doppler effect would need to be taken into account for interacting with the standing wave formed in the cavity. Using the above experimentally achievable parameters the approximations we have made in linearizing the dynamics of the system are valid, and the stability conditions derived by applying the Routh-Hurwitz criterion [40] are satisfied.

### III. GENERATION OF CAVITY-ASSISTED ATOM-FIELD ENTANGLEMENT

Figure 2 shows the correlations  $V_{12}$ ,  $V_{1a}$ , and  $V_{2a}$  as a function of the Fourier (measurement) frequency  $\omega$  (normalized to the cavity decay rate  $\kappa$ ) when the frequency detunings of the two cavity fields 1 and 2 with respect to the corresponding

input laser fields as well as the atomic 1–3 and 2–3 transitions are all equal to zero. In this case  $P_{1\text{in}} = P_{2\text{in}} = 1 \mu\text{W}$  and  $P_{\text{in}}^{\text{th}} = P_{1\text{in},2\text{in}}^{\text{th}} = 1.6 \times 10^{-5} \mu\text{W}$  so that the system is operating well above threshold. The normalization is such that these variances take the value of 2 at the shot noise limit, and  $V = 1$  represents 3 dB of noise suppression.  $V_{12}$  represents the correlation between the two output cavity fields, and  $V_{1a(2a)}$  represents the correlation between the output cavity field 1 (2) and the atoms, respectively. It can be seen that over a wide range of  $\omega$ ,  $V_{12}$  remains near 2 (the shot noise level), except that there exists a dip over a limited range (on the order of the cavity decay rate  $\kappa$ ) around zero Fourier frequency, with a minimum value of  $\approx 1.22$ , which demonstrates the generation of bipartite entanglement between the two output cavity fields in this regime. The correlations  $V_{1a}$  and  $V_{2a}$ , over nearly the entire range of the Fourier frequency  $\omega$ , are almost equal to 1, except for a dip within a limited range similar to that of  $V_{12}$  that appears around zero frequency, with the minimum values of  $\approx 0.80$  and  $\approx 0.56$ , respectively. These results demonstrate that the two output fields are both entangled with the atoms as well as with each other. Therefore, tripartite entanglement among the two cavity fields and the atoms can also be realized. Note that the higher degree of bipartite entanglement between the cavity field 2 and the atoms than that between cavity field 1 and the atoms is due to the parametric-type interaction of the cavity field 2 with the atoms and beam-splitter-type interaction between the cavity field 1 and the atoms. That is, every photon created in cavity field 2 is always accompanied by the annihilation of a photon in cavity field 1 and the creation of an atomic spin coherence excitation; a photon in cavity field 2 and an atomic spin coherence excitation are created simultaneously, similar to the twin beams in parametric down-conversion processes in nonlinear optical crystals. On the other hand, the creation of a photon in cavity field 1 is always accompanied by the annihilation of an atomic spin coherence excitation, which is analogous to a beam-splitter interaction.

Figure 3 presents the dependence of the correlations  $V_{12}$ ,  $V_{1a}$ , and  $V_{2a}$  at zero Fourier frequency as a function of the normalized input laser power  $P_{1\text{in}} = P_{2\text{in}} = P_{\text{in}}$  (normalized with respect to the threshold power  $P_{\text{in}}^{\text{th}} = P_{1\text{in},2\text{in}}^{\text{th}} = 1.6 \times 10^{-5} \mu\text{W}$  for the parameter values given above) of the two driving fields. Obviously,  $V_{12}$ ,  $V_{1a}$ , and  $V_{2a}$  have initial values far larger than 2 that decrease rapidly with the increase of the input laser power. When the input laser power is increased to the order of the threshold power  $P_{1\text{in},2\text{in}}^{\text{th}}$ ,  $V_{12}$ ,  $V_{1a}$ , and  $V_{2a}$  become smaller than 2, indicating the initially uncorrelated fields and atoms become entangled with each other. That is, field-field and field-atom entanglements can be realized with the  $\Lambda$ -type three-level atoms placed in an optical cavity operating above threshold. By further increasing the input laser power,  $V_{12}$ ,  $V_{1a}$ , and  $V_{2a}$  reach stable values of about 1.22, 0.80, and 0.56, respectively, and become insensitive to changes in the input field power, which is due to the fact that when the pumping rate  $\Gamma_i = g_{i3}^2 |\langle a_i \rangle|^2 / \gamma_i$  is far larger than  $\gamma_{12}$  (i.e., in the EIT regime), the quantum coherence  $\sigma_{12}$  saturates near its maximum value of  $-0.5$ , and stable values of the quantum correlations and entanglement are obtained. Similar behavior has also been studied in Ref. [20]. This indicates that with suitable cavity finesse  $F$  and atomic number  $N$ , bright

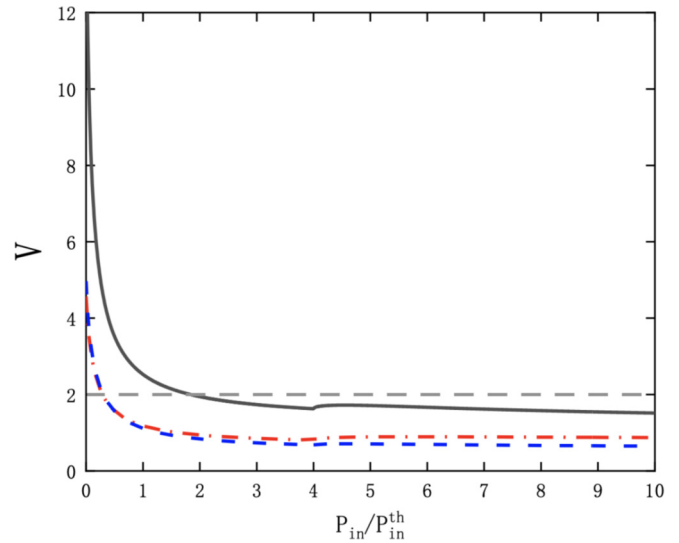


FIG. 3. The correlations  $V_{12}$  (solid black line),  $V_{1a}$  (dot-dashed red line), and  $V_{2a}$  (dashed blue line) at zero Fourier frequency as a function of the power  $P_{1\text{in}} = P_{2\text{in}}$  of the two input laser fields, normalized to the threshold power  $P_{\text{in}}^{\text{th}}$ . The other parameters are the same as those in Fig. 2. Below the horizontal gray dashed line the variance is sub-shot-noise. The small features appearing near  $P_{\text{in}}/P_{\text{in}}^{\text{th}} = 4$  are discussed in the text.

entangled output optical fields as well as light-atom tripartite entanglement can be obtained with this cavity-assisted atomic system. As discussed in Ref. [21], the noise compression or squeezing in the EPR-type operator criteria [36] is a sufficient condition for a successful teleportation of a quantum state between two sites [41].

In Fig. 3 the atom-field correlations  $V_{1a}$  and  $V_{2a}$  are seen to behave almost identically below the threshold pump power, but the different type of atom-field interactions cause them to deviate from each other above the pump threshold, as discussed above. A more curious feature is that there is a noticeable change in the field-field correlation  $V_{12}$  at a value of  $P_{\text{in}}/P_{\text{in}}^{\text{th}} = 4$ . Sharp features in the field-field correlations also appear in an OPO driven above threshold at similar pump values in [20,42]. The OPO configuration is similar to what we have here, with a driven medium in a cavity, and in those cases the features were interpreted as a signature of pump depletion. The feature in  $V_{12}$  here is presumably also related to the onset of pump depletion.

It is well known that the cooperativity parameter  $C$ , which quantifies the collective atom-field interaction in an optical cavity, plays a key role in the generation of atom-field squeezing or entanglement [5,22,23]. Figure 4 shows three-dimensional (3D) plots of the correlations  $V_{12}$ ,  $V_{1a}$ , and  $V_{2a}$  at zero Fourier frequency with respect to the cavity finesse  $F$  and atomic number  $N$ . As seen from Figs. 4(a)–4(c), when either the cavity finesse or the atomic number is very small, the correlations  $V_{12}$ ,  $V_{1a}$ , and  $V_{2a}$  are nearly equal to 2, 1, and 1, respectively, indicating that although there exists entanglement between the atoms and the two output cavity fields, no bipartite entanglement between the two output fields is created. With the increase of the cavity finesse and/or atomic number, the correlations  $V_{12}$ ,  $V_{1a}$ , and  $V_{2a}$  become smaller than

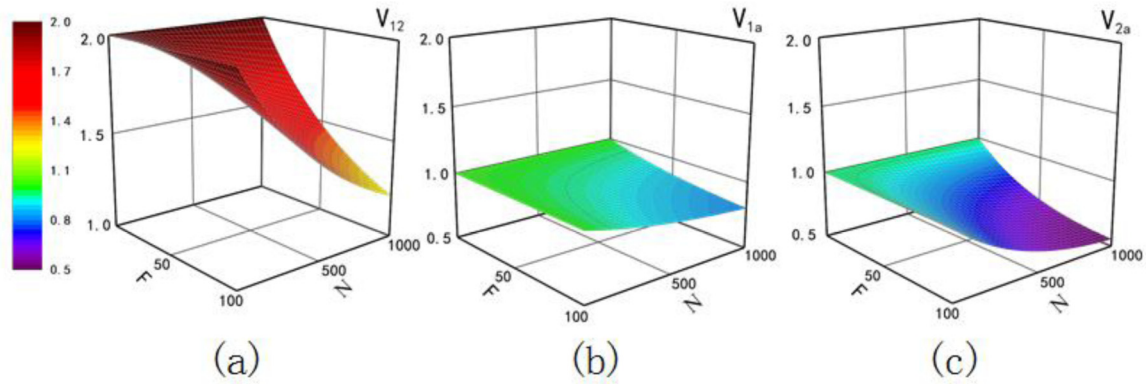


FIG. 4. 3D plots of the correlation parameters  $V_{12}$  (a),  $V_{1a}$  (b), and  $V_{2a}$  (c) at zero Fourier frequency with respect to the cavity finesse  $F$  and the atomic number  $N$ . The other parameters are the same as those in Fig. 2. (Each axis is a number without units.) The color bar on the left gives the scale for the values of the correlation parameters.

2, 1, and 1, respectively, implying the generation of bipartite entanglement between the two output cavity fields, as well as an enhancement of the degree of entanglement between the two output fields and the atoms. Within the experimentally feasible parameter range, as well as under the above adiabatic approximation, the larger the cavity finesse  $F$  and/or atomic number  $N$ , the stronger the bipartite entanglement that is generated between the two output cavity fields and the atoms.

#### IV. MECHANISM OF CAVITY-ASSISTED ATOM-FIELD ENTANGLEMENT

The strong bipartite entanglement between the two output cavity fields and between the fields and the atoms can be understood by considering the interaction between the cavity fields and the atoms. It is easy to deduce from Eqs. (2a)–(2e) that in the adiabatic approximation, by replacing the optical coherences  $\sigma_{13}$  and  $\sigma_{23}$  with their steady-state values, the effective interaction Hamiltonian of the atom-field hybrid system can be described by  $H_I = -\frac{i2\hbar g_{13}g_{23}\sqrt{N}}{\gamma_1+\gamma_2}a_1a_2^\dagger\sigma_{21} + \text{H.c.}$  This interaction clearly indicates that every photon created in cavity field 2 is always accompanied by the annihilation of a photon in cavity field 1 and the creation of an atomic spin coherence excitation; that is, the cavity field 1 is quantum anticorrelated with the cavity field 2 as well as the atomic spin coherence. Note that the atomic interaction is not symmetric in the two cavity fields in that there is a creation of spin coherence along with phonons created in cavity field 2, while there is an annihilation of spin coherence with the photons created in cavity field 1. Strong tripartite entanglement among the two cavity fields and the atoms can be achieved. This is similar to the parametric down-conversion process for generating pump-signal-idler three-color entanglement by using an OPO [7,8]. It should be noted that in Ref. [31], the authors examined the quantum correlations at a fixed analysis frequency and showed that there exist quantum correlations (anticorrelations) between the amplitude (phase) quadratures of the pump and probe fields, which is distinct from the current quantum correlation relationship between the output fields.

As seen in Eqs. (2a)–(2e), due to the quantum coherence  $\sigma_{12}$  between the atomic lower doublet induced by the two cavity fields, the two cavity field modes are coupled with each other and subsequently correlation and entanglement between them can be established. If there were no quantum coherence,  $\sigma_{12}$ , the existence of the atoms would only influence the effective detunings and decay rates of the two cavity fields and there would be no mutual coupling between the two cavity fields, and no entanglement could be established between them. In addition, as seen from Eq. (2c), the atomic spin coherence operator is a linear superposition of the two cavity field operators, which implies that the atomic spin coherence inherently gets entangled with both of the cavity fields. This shows that the entanglement between the two cavity fields and the atoms should exist in the whole range of the Fourier frequencies in Fig. 2.

In comparison to the four-wave mixing technique of Ref. [10] the ultimate entanglement between the fields that can be obtained with the present technique is not any larger, but the light power levels required are drastically reduced by the use of the cavity in this case. Using a cold atom system is perhaps a practical disadvantage here, but the use of hot atoms could also be investigated.

Recently up to  $-1.5$  dB of quantum field-field anticorrelations (corresponding to  $V \approx 0.71$ ) have been observed in an experiment that is somewhat similar to the one described here, but does not include a cavity [43]. The experiments involve similarly competing processes that can be described as Raman processes coupled through an exchange of atomic spin coherence in a vapor, and demonstrate the attainability of the needed experimental parameters.

In conclusion, we have shown that field-field and field-atom entanglements can be achieved in an optical cavity containing  $\Lambda$ -type three-level atoms in the above-threshold regime. Due to the cavity-induced atom-field cooperative coupling, entanglement between two bright output cavity fields as well as entanglement of the fields with the atoms can be achieved with realistic experimental parameters. This atom-cavity hybrid system provides a convenient and efficient platform for producing bright nondegenerate entangled fields as well as atom-light multipartite entanglement by using only

coherent input laser fields, and may find promising applications in quantum information processing and networking protocols. Further investigation into the possibility of doing similar experiments with hot atoms, which would simplify the experimental arrangements, is needed.

### ACKNOWLEDGMENTS

This work is supported by China Scholarship Council (Grant No. 201906895012), National Natural Science Foundation of China (Grant No. 12174243), National Science Foundation Grant No.1708036, and the Air Force of Scientific Research Grant No. FA9550-16-1-0423.

### APPENDIX

In the derivation of Eq. (4), we consider the frequency detunings of the two cavity fields  $E_i$  with respect to the corresponding input laser fields (and the atomic 1–3 and 2–3 resonant transitions) all equal to zero (EIT configuration), and

we assume that the optical coherences  $\sigma_{13}$  and  $\sigma_{23}$  adiabatically follow the ground-state observables. In this case, the mean values of  $\sigma_{13}$  and  $\sigma_{23}$  are pure imaginary numbers, and from Eqs. (2a)–(2e), together with  $\langle\sigma_{11}\rangle + \langle\sigma_{22}\rangle + \langle\sigma_{33}\rangle = N$ , we obtain the following equations,

$$-\kappa_1 \langle a_1 \rangle^2 + E_1 \langle a_1 \rangle - \gamma_{13} \langle \sigma_{33} \rangle = 0, \quad (\text{A1})$$

$$-\kappa_2 \langle a_2 \rangle^2 + E_2 \langle a_2 \rangle - \gamma_{23} \langle \sigma_{33} \rangle = 0, \quad (\text{A2})$$

$$(\gamma_1 + \gamma_2) \langle \sigma_{33} \rangle [\gamma_{12} \gamma_{13} + g^2 (\langle a_1 \rangle^2 + \langle a_2 \rangle^2)] - 4g^2 \gamma_{12} (N - 3 \langle \sigma_{33} \rangle) \frac{\langle a_1 \rangle^2 \langle a_2 \rangle^2}{\langle a_1 \rangle^2 + \langle a_2 \rangle^2} = 0, \quad (\text{A3})$$

$$\langle a_1 \rangle^2 (\langle \sigma_{11} \rangle - \langle \sigma_{33} \rangle) - \langle a_2 \rangle^2 (\langle \sigma_{22} \rangle - \langle \sigma_{33} \rangle) = 0, \quad (\text{A4})$$

under the conditions that  $P_{1\text{in}} = P_{2\text{in}}$ ,  $g_{i3}^2 \langle a_i \rangle^2 / \gamma_{i3} \gamma_{12} \gg 1$ , and  $\frac{2\kappa \langle a_i \rangle^2}{N \gamma_{12}} \gg \frac{1}{C_i}$ , with the cooperativity parameter  $C_i = g_{i3}^2 N / \kappa \gamma_i$ , we find  $\langle a_i \rangle = (E_i \pm \sqrt{E_i - \kappa N \gamma_{12}}) / 2\kappa$ .

- 
- [1] P. van Loock and S. L. Braunstein, *Phys. Rev. Lett.* **84**, 3482 (2000).
  - [2] E. Knill, R. Laflamme, and G. J. Milburn, *Nature (London)* **409**, 46 (2001).
  - [3] T. Aoki, N. Takei, H. Yonezawa, K. Wakui, T. Hiraoka, A. Furusawa, and P. van Loock, *Phys. Rev. Lett.* **91**, 080404 (2003).
  - [4] P. van Loock and A. Furusawa, *Phys. Rev. A* **67**, 052315 (2003).
  - [5] A. Heidmann, R. J. Horowicz, S. Reynaud, E. Giacobino, C. Fabre, and G. Camy, *Phys. Rev. Lett.* **59**, 2555 (1987).
  - [6] S. L. Braunstein and P. van Loock, *Rev. Mod. Phys.* **77**, 513 (2005).
  - [7] A. S. Villar, M. Martinelli, C. Fabre, and P. Nussenzveig, *Phys. Rev. Lett.* **97**, 140504 (2006).
  - [8] A. S. Coelho, F. A. S. Barbosa, K. N. Cassemiro, A. S. Villar, M. Martinelli, and P. Nussenzveig, *Science* **326**, 823 (2009).
  - [9] A. Kuzmich, W. P. Bowen, A. D. Boozer, A. Boca, C. W. Chou, L. M. Duan, and H. J. Kimble, *Nature (London)* **423**, 731 (2003).
  - [10] V. Boyer, A. M. Marino, R. C. Pooser, and P. D. Lett, *Science* **321**, 544 (2008).
  - [11] A. M. Marino, R. C. Pooser, V. Boyer, and P. D. Lett, *Nature (London)* **457**, 859 (2009).
  - [12] N. Sangouard, C. Simon, H. de Riedmatten, and N. Gisin, *Rev. Mod. Phys.* **83**, 33 (2011), and references therein.
  - [13] X. H. Yang, Y. Y. Zhou, and M. Xiao, *Phys. Rev. A* **85**, 052307 (2012).
  - [14] X. H. Yang and M. Xiao, *Sci. Rep.* **5**, 13609 (2015).
  - [15] K. Zhang, W. Wang, S. Liu, X. Pan, J. Du, Y. Lou, S. Yu, S. Lv, N. Treps, C. Fabre, and J. Jing, *Phys. Rev. Lett.* **124**, 090501 (2020).
  - [16] D. Vitali, S. Gigan, A. Ferreira, H. R. Böhm, P. Tombesi, A. Guerreiro, V. Vedral, A. Zeilinger, and M. Aspelmeyer, *Phys. Rev. Lett.* **98**, 030405 (2007).
  - [17] M. Aspelmeyer, T. J. Kippenberg, and F. Marquardt, *Rev. Mod. Phys.* **86**, 1391 (2014), and references therein.
  - [18] X. H. Yang, Z. Y. Yin, and M. Xiao, *Phys. Rev. A* **99**, 013811 (2019).
  - [19] L. Hilico, C. Fabre, S. Reynaud, and E. Giacobino, *Phys. Rev. A* **46**, 4397 (1992).
  - [20] A. Montaña Guerrero, P. Nussenzveig, M. Martinelli, A. M. Marino, and H. M. Florez, *Phys. Rev. Lett.* **125**, 083601 (2020).
  - [21] B. A. F. Ribeiro, R. B. de Andrade, M. Martinelli, and B. Marques, *Phys. Rev. A* **102**, 023522 (2020).
  - [22] A. Dantan and M. Pinard, *Phys. Rev. A* **69**, 043810 (2004).
  - [23] A. Dantan, A. Bramati, and M. Pinard, *Europhys. Lett.* **67**, 881 (2004).
  - [24] L. M. Duan, M. D. Lukin, J. I. Cirac, and P. Zoller, *Nature (London)* **414**, 413 (2001).
  - [25] Z. S. Yuan, Y. A. Chen, B. Zhao, S. Chen, J. Schmiedmayer, and J. W. Pan, *Nature (London)* **454**, 1098 (2008).
  - [26] R. Zhang, S. Garner, and L. V. Hau, *Phys. Rev. Lett.* **103**, 233602 (2009).
  - [27] U. Schnorrberger, J. Thompson, S. Trotzky, R. Pugatch, N. Davidson, S. Kuhr, and I. Bloch, *Phys. Rev. Lett.* **103**, 033003 (2009).
  - [28] C. Schori, B. Julsgaard, J. L. Sorensen, and E. S. Polzik, *Phys. Rev. Lett.* **89**, 057903 (2002).
  - [29] C. L. Garrido-Alzar, J. G. Aguirre Gómez, L. S. Cruz, M. França Santos, and P. Nussenzveig, *Europhys. Lett.* **61**, 485 (2003).
  - [30] L. S. Cruz, D. Felinto, J. G. Aguirre Gómez, M. Martinelli, P. Valente, A. Lezama, and P. Nussenzveig, *Eur. Phys. J. D* **41**, 531 (2007).
  - [31] C. L. Garrido-Alzar, M. Franca Santos, and P. Nussenzveig, *arXiv:quant-ph/0205119*.
  - [32] K. Hammerer, A. S. Sørensen, and E. S. Polzik, *Rev. Mod. Phys.* **82**, 1041 (2010).
  - [33] A. Dantan, A. Bramati, and M. Pinard, *Phys. Rev. A* **71**, 043801 (2005).
  - [34] K. Dechoum, M. D. Hahn, R. O. Vallejos, and A. Z. Khoury, *Phys. Rev. A* **81**, 043834 (2010).

- [35] K. V. Kheruntsyan and K. G. Petrosyan, *Phys. Rev. A* **62**, 015801 (2000).
- [36] L. M. Duan, G. Giedke, J. I. Cirac, and P. Zoller, *Phys. Rev. Lett.* **84**, 2722 (2000).
- [37] Q. Glorieux, R. Dubessy, S. Guibal, L. Guidoni, J. P. Likforman, and T. Coudreau, *Phys. Rev. A* **82**, 033819 (2010).
- [38] M. D. Reid, *Phys. Rev. A* **40**, 913 (1989).
- [39] G. Hernandez, J. Zhang, and Y. Zhu, *Phys. Rev. A* **76**, 053814 (2007).
- [40] E. X. DeJesus and C. Kaufman, *Phys. Rev. A* **35**, 5288 (1987).
- [41] A. Furusawa, J. Sørensen, S. Braunstein, C. Fuchs, H. J. Kimble, and E. S. Polzik, *Science* **282**, 706 (1998).
- [42] C. Fabre, E. Giacobino, A. Heidmann, and S. Reynaud, *J. Phys.* **50**, 1209 (1989); C. Fabre, E. Giacobino, A. Heidmann, L. Lugiato, S. Reynaud, M. Vadaracchino and W. Kaige, *Quantum Opt.* **2**, 159 (1990); G. Bjork and Y. Yamamoto, *Phys. Rev. A* **37**, 125 (1988).
- [43] X. Yang, N. Brewer, and P. Lett (unpublished).